Experimental Investigation of the Equlibria in Mg-Al-(Ca,Sr) Systems

M.A.Parvez[1], X. Wang[1], E. Essadiqi[2], M. Medraj[1]

[1]Concordia University, Montreal, Canada
[2]CANMET-MTL, Ottawa, Canada

Keywords: Mg-Al alloys, Phase diagram, DSC, XRD, Thermodynamic modeling.

Abstract

The phase diagrams of Mg-Al-Sr and Mg-Al-Ca systems were investigated experimentally by differential scanning calorimetry (DSC) and X-ray diffraction (XRD) techniques. The experimental work focused on the critical regions after reviewing the phase diagrams developed by thermodynamic modeling. DSC has permitted real time measurement of the phase changes involved in these systems. The temperature ranges for the phase change peaks have been determined. Enthalpy of melting and enthalpy of formation of the compounds are also reported. Comparison between these results and the thermodynamic findings will be discussed. These results along with the XRD analysis are used to establish the equilibria in Mg-Al-Sr and Mg-Al-Ca systems. XRD was used to identify the phases in the studied samples. Al_4Sr and Al_2Ca were found to be the dominating phases in Mg-Al-Sr and Mg-Al-Ca systems, respectively.

Introduction

Magnesium has the best strength to weight ratio of common structural metals and has exceptional die-casting characteristics [1]. This makes magnesium alloys one of the most promising light-weight materials for automotive application. To date, most Mg applications in the auto industry are in the form of die-cast parts applications. However, wrought magnesium applications, particularly sheet, and powertrain applications represent tremendous growth opportunities for magnesium. Unfortunately, magnesium alloys face a challenge for powertrain applications because of their limited creep resistance at higher temperatures [2].

Calcium and strontium can benefit the magnesium alloys for both applications. The ductility of magnesium increases as temperature increases [3]. It is well known that the addition of Ca up to 0.3% increases ductility through grain size reduction [4]. Strontium like calcium is a very effective grain refiner [5,6].

In recent years Mg-Al(Sr,Ca) have emerged as potential heat-resistant Mg-alloys. The development of Mg-Al-(Sr,Ca) was aimed to replace RE additions to Mg alloys. One of the main challenges of these alloy systems is to optimize the combinations of properties such as creep resistance, tensile yield strength and castability [7,8].

However, to date, little effort has been made to construct the phase relationships of Mg-Al-Sr and Mg-Al-Ca systems. Mg-Al-Sr was modeled by Chartrand et al. in 1980's and investigated experimentally by Makhmudov et al. [9,10]. The calculated phase diagram exhibited substantial disagreement with the experimental data. The ternary system was modeled without using ternary phases or ternary interaction parameters. In 2003, Koray et al. modeled Mg-Al-Sr, and obtained results very similar to Chartrand et al. except for the extent of the Mg_2Sr field [11]. Baril et al. [12] recently investigated five samples of the Mg-Al-Sr system in the Mg-rich region. They observed distinct peaks in the XRD pattern for one of the samples. This phase is tentatively designated as $Al_3Mg_{13}Sr$ which is however detrimental to the tensile strength and ductility.

In the Mg-Al-Ca system, Gröbner et al. [13] performed thermodynamic calculations of the phase diagram on the basis of the three binary subsystems whereas experimental investigations were carried out by DTA and X-ray powder diffraction analysis. In this investigation, a consistent thermodynamic modeling of the ternary system was done involving the substantial ternary solid solubilities. Koray et al. [14] calculated the ternary Mg-Al-Ca diagram by combining the data of the three binary systems, Al-Mg, Ca-Mg, and Al-Ca, assuming no ternary solubility in the binary compounds along with no ternary interactions. Powell et al. [15] suggested the presence of a ternary solid solution phase in this system. Recent investigations [16] pointed out that Al_2Ca and $CaMg_2$ are the primary precipitates responsible for the improvement of creep resistance in this system. However, the composition ranges for the formation of these precipitates differ drastically from one researcher to another. For instance, Gröbner et al. [13] reported that it is possible to form $CaMg_2$ with up to 32 at% Al, whereas Koray et al. [14] reported only 18 at% Al.

The considerable discrepancy among the published results and the lack of experimental data demands new investigation for these systems. In this work, the phase equilibria in Mg-Al-(Ca,Sr) systems were studied experimentally. A comparison with the thermodynamic calculations is also presented.

Experimental Procedures

Thermal analytical investigation and phase identification were carried out in the Mg-rich region of the Mg-Al-Sr and Mg-Al-Ca systems. The alloys were prepared at CANMET. The nominal compositions for the samples for each system are given in Table 1. The samples were analyzed chemically and the nominal sample compositions remained in very close proximity with the actual compositions.

Table 1: Nominal compositions of the studied alloys

Mg-Al-Sr alloy	Wt.% of Sr	Wt.% of Mg	Wt.% of Al
Sample 1	23.75	53.75	22.5
Sample 2	3.5	88.5	8
Mg-Al-Ca alloy	Wt.% of Ca	Wt.% of Mg	Wt.% of Al
Sample 3	4.5	78	17.5
Sample 4	23.4	44	32.6

In preparing the Mg-Al-Sr alloys, magnesium of 99.8 wt%, aluminum of 99.9 wt.% and strontium of 99 wt.% were used whereas for Mg-Al-Ca, calcium of 99 wt.% was used. The charge was melted in a graphite crucible in an induction melting furnace under argon with 1%SF6 to protect the melt from oxidation.

Thermal investigation of the systems was performed using a Setaram Setsys DSC-1200 instrument. Temperature calibration of the DSC equipment was done using standard samples of Al and minimal thermal lag was observed. The samples were cut and mechanically polished to remove any possible contaminated surface layers. Afterwards, they were cleaned with acetone and placed in a graphite crucible with a lid cover to prevent chemical reactions with Mg vapors. To avoid oxidation, multiple evacuations followed by rinses with argon were done. In thermal analysis by DSC, selection of crucibles, the dimensions of the sample as well as the heating and cooling rates are important. The DSC measurements were carried out under flowing argon atmosphere with heating and cooling rates of 5°C/min. Slower heating rates do not reveal any other thermal arrests. The weight of the sample was 40~50 mg. The reproducibility of every measurement was confirmed by collecting the data during three heating and cooling cycles. Temperatures along with enthalpies corresponding to various thermal events were obtained from the analysis of the DSC curves during heating and cooling runs. However, the solidification behavior can be revealed much better with a cooling scan.

Phase identification was carried out by X-ray diffraction (XRD). All the samples were investigated in the powder form in the as-cast condition. The measurement was performed with a Philips diffractometer (Cu$K\alpha$ radiation) equipped with a PW 1050/25 focusing gonimometer with steps 0.02° of 2θ diffraction angle range and 1s exposure time. PowderCell 2.1 was used to analyze the diffraction patterns [17].

Results and Discussions

Experimental investigation was carried out using DSC and XRD on Mg-Al-(Ca,Sr) systems. Twenty different ternary samples were studied in each system. However, in this paper, only two compositions for each system will be discussed. The evolution of phase transformations as a result of temperature increase was followed by obtaining DSC data in the selected temperature ranges. Also cooling was conducted with similar scanning rate to detect the crystallization as well as the stability of the phase.

1. Mg-Al-Sr

DSC spectra of sample 1 with heating and cooling runs are shown in Fig. 1. The onset temperature, peak temperature, melting temperature and the melting enthalpy were registered. It shows two peaks during heating and three peaks during cooling. Similar results were observed in all the three heating and cooling cycles. It

can be seen from this figure that there is a temperature difference between the heating and cooling patterns, however the maximum temperature difference of the observed signals between two repetitive heating or cooling runs were below 12°C. The enthalpy and onset temperatures were determined after the subtraction of the baseline. The onset temperature during cooling was about 2°C below the onset temperatures observed in the heating process. On heating, onset temperature was used for invariant reactions while peak maximum was used for phase field boundaries. On cooling, onset temperature was used for both the invariant reactions and the phase field boundaries.
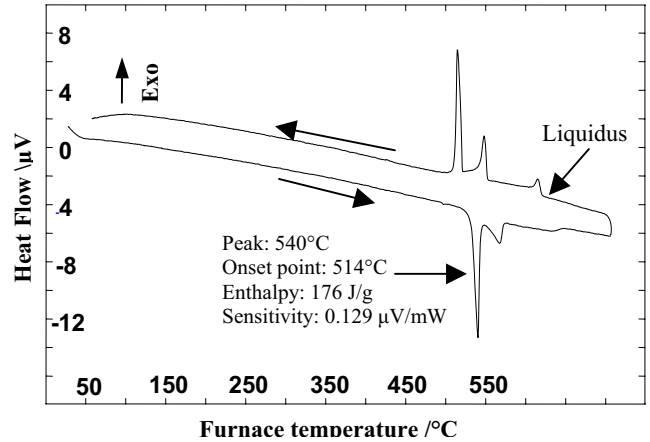

Figure 1: DSC spectra of sample 1 (23.9 wt.% Sr, 53.75 wt.% Mg and 22.5 wt.% Al) during heating and cooling.

During heating of this sample, two thermal arrests, corresponding to the invariant equilibrium at 514°C and the univariant equilibrium at 560°C are observed. The 1st peak is high and sharp and resembles a δ function. So it denotes the peak of eutectic melting. The second peak is a non-isothermal transition (univariant) as it exhibits a peak, which is lower and broader. For this sample, the liquidus temperature is observed during cooling which is 614°C. The size of the freezing signals is increased due to supercooling.
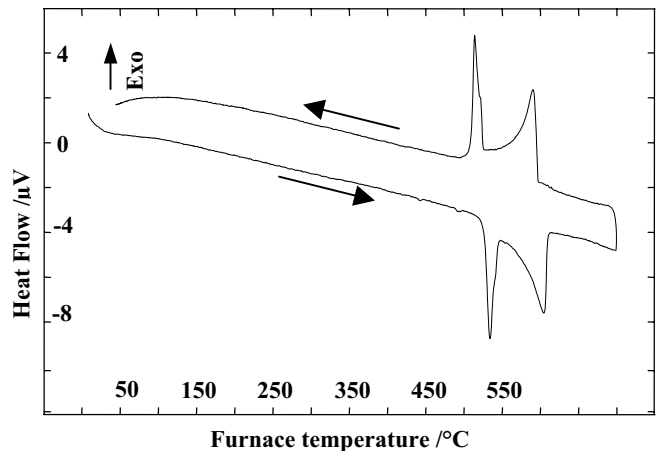

Figure 2: DSC spectra of sample 2 (3.5 wt.% Sr, 88.5 wt.% Mg and 8 wt.% Al) with heating and cooling runs.

Figure 2 shows the DSC spectra of sample 2, where two peaks in both heating and cooling cycles can be observed. The difference in onset temperature between heating and cooing cycle was found about 4°C.

In this sample, the endothermic peak during heating begins at 500°C. The absence of a single endothermic peak without any tail indicates that this sample does not melt congruently but undergoes a peritectic decomposition at 550°C. On cooling, the onset temperatures of the first and second exothermic peaks are observed at 525°C and 597°C. The second peak exhibits a small tailing. The liquidus temperature was registered at 605°C. Table 2 summarizes the parameters of melting for the two Mg-Al-Sr samples where the sensitivity is 0.129 µV /mW.

Table 2: *Parameters of melting for the two Mg-Al-Sr samples (c: denotes cooling).*

Sample	Onset Temp. °C (Peak 2)	Enthalpy of melting J/g	Liquidus Temp. °C
1	550c	101.52	614
2	597c	249.4	605

XRD was used to confirm the phase identification of the Mg-Al-Sr-based alloys in the as-cast condition. PowderCell was used to analyze the diffraction patterns. The peaks are identified by markers given in the legend of each figure.
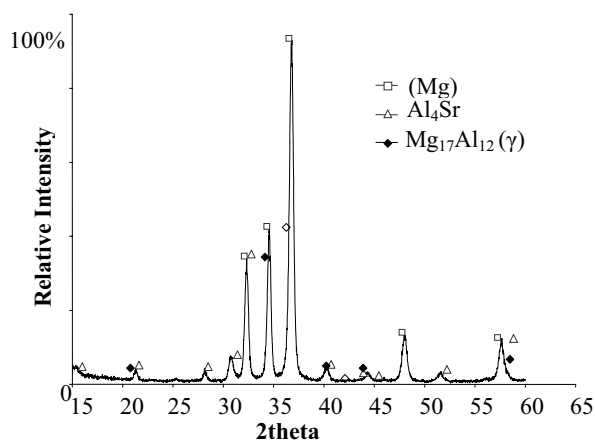

Figure 3: *X-ray diffraction pattern of sample 1 (23.9 wt.% Sr, 53.75 wt.% Mg and 22.5 wt.% Al)*

In sample 1, three phases were identified in the diffraction pattern. It can be seen from Fig. 3 that this sample is composed of (Mg), Al_4Sr and $Mg_{17}Al_{12}$ (γ) at room temperature. (Mg) peaks are identified as a hexagonal unit cell (space group $P6_3$/mmc, a = 3.1210Å and c = 5.1581Å), while Al_4Sr and $Mg_{17}Al_{12}$ were identified using a tetragonal unit cell (space group I_4/3m, a = 11,07Å) and (space group I_4/3m, a = 10.5438 Å), respectively. The patterns were checked with known oxide phases such as MgO, Al_2O_3 and $MgAl_2O_4$ for any possible oxide formation. The XRD pattern showed no trace for any additional phase. Baril et al. [8] reported an alloy with the chemical composition of 2.4 wt.% of Sr, 91.6 wt.% of Mg and 6.0 wt.% of Al, which is very close to this sample, without $Mg_{17}Al_{12}$. This information along with some more experimental data with different samples in this Mg-rich region can be used to setup a window to identify the possible

creep resistant alloy for the end user. Because it is very important to make an alloy without $Mg_{17}Al_{12}$, which is detrimental to tensile strength, creep and ductility.
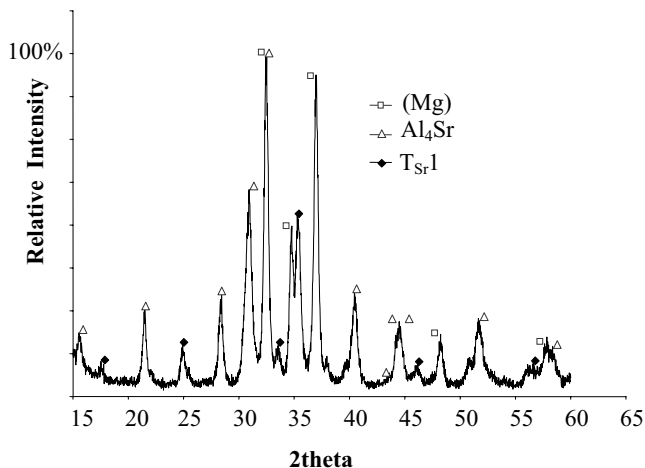

Figure 4: *X-ray diffraction pattern of sample 2 ((3.5 wt.% Sr, 88.5 wt.% Mg and 8 wt.% Al).* $T_{Sr}1$ denotes ternary intermetallic or solid solution

In the XRD pattern of sample 2 (Fig.4), distinct peaks associated with (Mg) and Al_4Sr are observed. There is no information regarding any stable ternary compounds available. Some of the peaks of the XRD pattern for this sample did match well with a ternary compound tentatively designated as $Al_3Mg_{13}Sr$ but only within 40° diffraction angle range. However, the crystal structure of $Al_3Mg_{13}Sr$ is still unknown. So this intermetallic phase, tentatively designated as $T_{Sr}1$, may be a new ternary compound or a ternary solid solution. It is very important to note that these peaks also appear in the XRD patterns of other samples which are in very close proximity to this composition in the ternary Mg-Al-Sr system. In this system, Al_4Sr was found to be the dominating phase for most of the samples.
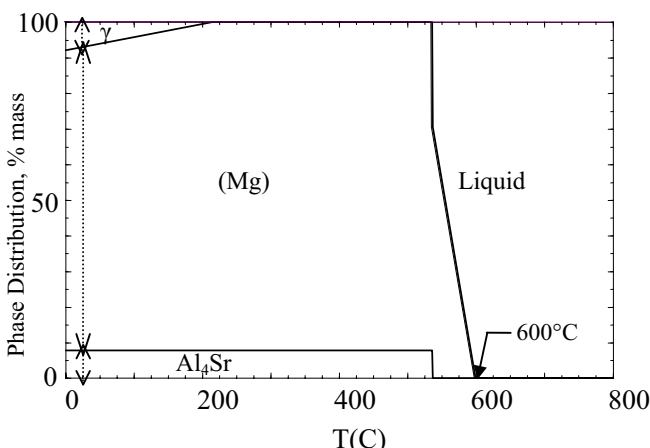

Figure 5: *Phase assemblage diagram of sample 1.*

The experimental results were compared with the thermodynamic calculations to confirm the phase identification. With the given experimental compositions and conditions, the stable phases were predicted using FactSage and the database developed by Chartrand et al. [9].

Fig. 5 shows the phase assemblage diagram of sample 1 where the relative mass versus temperature is calculated. The proportion of each phase at any temperature of interest can easily be interpreted from this figure. For instance, at 25°C, 100 g of the overall material consists of 8g of Al_4Sr, 6g of $Mg_{17}Al_{12}$ (γ) and 86g of (Mg). The proportion of each phase for this sample has been reflected in terms of peak intensity in the diffraction pattern. Moreover, the thermodynamic prediction is consistent with DSC result. It can be seen that the liquidus temperature of this sample is 600°C, whereas according to the DSC results the liquidus temperature is about 614°C. The summary of DSC results compared with the calculated values and the phase field boundary are presented in Table 3

Table 3: *DSC measurements with thermodynamic analysis of Mg-Al-Sr alloys (h: denotes heating and c: denotes cooling).*

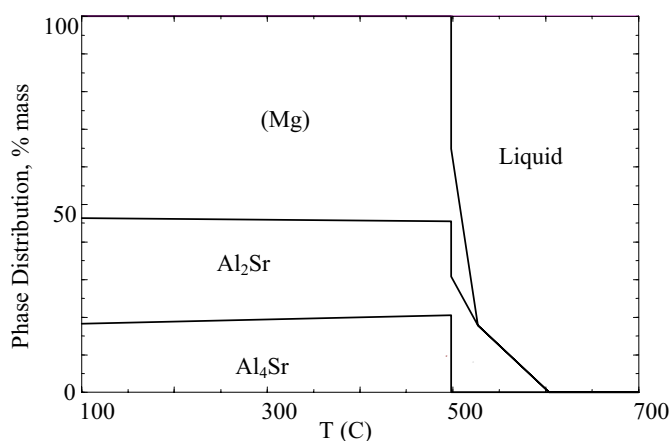| Sample	DSC Thermal Signals(°C)	Thermodynamic Prediction [Ref.9]	
		Temp.	Reaction or phase boundary
1	614 c	600	L / L+(Mg)
	550C/560h		
	515 C/514h	520	L+ (Mg) / (Mg)+Al_4Sr
		200	(Mg)+Al_4Sr / (Mg)+Al_4Sr +γ
2	605c	610	L / L+ Al_2Sr
	597c/600h	540	L+ Al_2Sr / (Mg)+Al_2Sr
	525c/523h	499	(Mg)+Al_2Sr / (Mg)+Al_4Sr +Al_2Sr

Figure 6: *Phase assemblage diagram of sample 2.*

The phase assemblage versus temperature of sample 2 is presented in Fig. 6. While cooling from melt, calculations predict that Al_2Sr solidifies first, followed by (Mg). Thermodynamic calculations also show that the Al_4Sr precipitates at 500°C. However, the sample does not show any Al_2Sr phase in XRD pattern and shows some unknown peaks. DSC measurements and calculated thermal arrests are presented in Table 3.

2. **Mg-Al-Ca**

DSC data provided the temperature and position of the invariant and univarant reactions existing in the investigated compositions. Fig. 7 shows the DSC spectra of sample 3 during heating and cooling scans. There are two thermal events that can be observed in the heating spectrum. They are registered at 443°C and 555°C with two predominant endothermic peaks. The 1st peak is sharp and narrow, which indicates an isothermal transition. The heat capacity change is infinite in this phase. The onset temperature during cooling was about 5°C lower than the onset temperature observed during heating cycle. In this sample, the liquidus temperature is at 550°C. The enthalpy of melting for this sample was registered as 248 J/g.
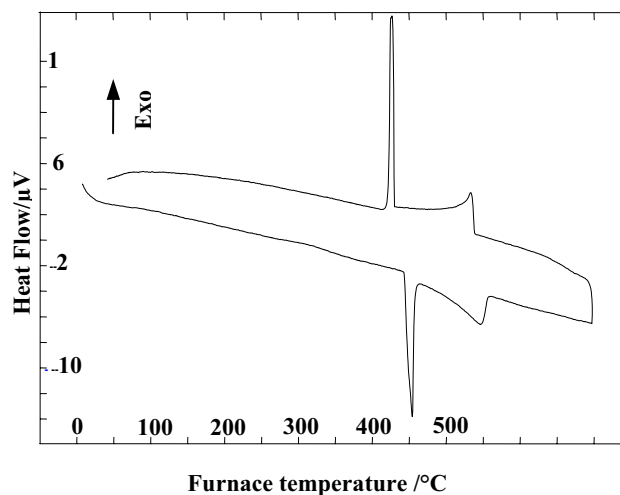

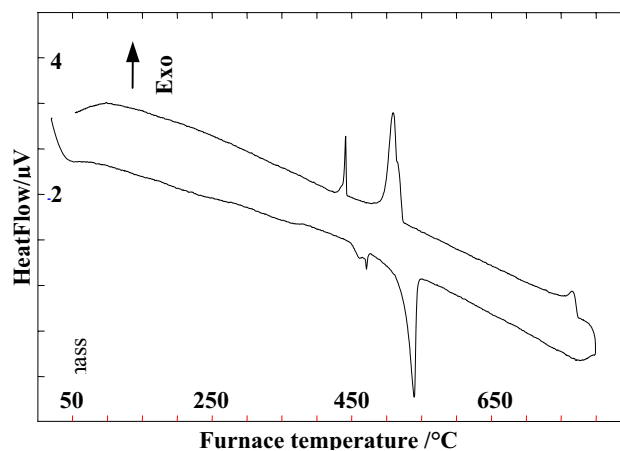**Figure 7:** *DSC spectra of sample 3 (4.5 wt.% Ca, 78 wt.% Mg and 17.5 wt.% Al).*

Figure 8: *DSC spectra of sample 4 (23.4 wt.% Ca, 44 wt.% Mg and 32.6 wt.% Al).*

DSC spectra of sample 4 are plotted in Fig. 8. In this sample, during heating, the first endothermic peak begins at 443°C. The size of the 1st signal during cooling is increased due to supercooling. These results are reproduced three times. Slower heating rates do not reveal any other thermal arrests. Table 4 summarizes the parameters of melting for the two Mg-Al-Ca samples. The liquidus temperature increases with decreasing aluminum and calcium concentrations. The temperature ranges of the phase transformations were determined during heating and cooling cycles.

Table 4: *Parameters of melting for the two Mg-Al-Ca samples (c: denotes cooling).*

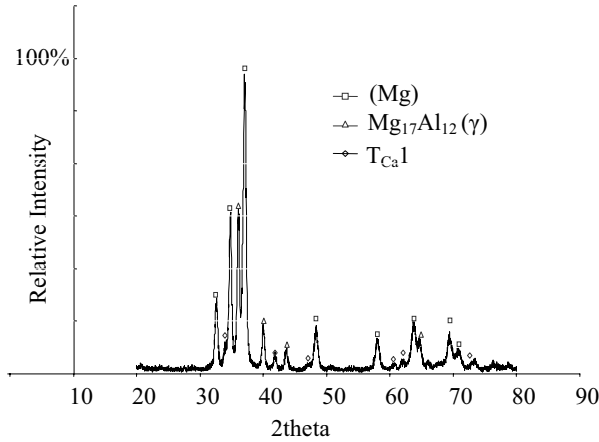| Sample	Onset Temp. °C (Peak 2)	Enthalpy of melting J/g	Liquidus Temp. °C
3	550c	248	550
4	523c	159	760

Figure 9: *X-ray diffraction patterns of sample 3.* $T_{Ca}1$ denotes ternary intermetallic or solid solution.

XRD was used to identify the phases in the ternary Mg-Al-Ca system. XRD pattern of sample 3 at room temperature is shown in Fig.9. Two phases were identified as (Mg) and γ. Some unknown peaks have been observed that are not matching any known phases in the ternary Mg-Al-Ca system. However, the large solubilities of Al_2Ca, Al_3Ca_8 and Mg_2Ca have complicated the identification of these binary phases. Gröbner et al. [13] reported rod-like primary crystallizing phases with variable composition in between Mg_2Ca and Al_2Ca. But instead of interpreting as a ternary phase with large homogeneity range it is being attributed to the large solubility of Al_2Ca and Mg_2Ca. Koray [14] et al., however, suggested that this intermetallic phase is a ternary solid solution phase in the hexagonal Mg_2Ca structure. In the future work, some more samples nearby this composition will be studied to resolve this inconsistency and identify the phase.

On the other hand, all the peaks of sample 4 were identified. The phases at room temperature are (Mg), Al_2Ca and $Mg_{17}Al_{12}$ (γ). It is important to completely remove the γ phase for high temperature applications. It can be seen from Fig. 10 that the intensity of γ peak is very low, which suggests that very careful selection of compositions should help the end users to avoid γ phase formation nearby this sample. In general, Al_2Ca was found to be the dominating phase in the investigated compositions.

The phase assemblage diagram of sample 3 is shown in Fig. 11. The stable phases were predicted using the database developed by Islam [18]. It can be seen from the figure that the proportion of γ phase is very low, which is being reflected in the XRD pattern in terms of peak intensity. The calculated liquidus temperature for this sample is 530°C. However, according to the DSC results, the liquidus temperature is 550°C. This discrepancy may be due to the fact that the thermodynamic model is optimized without taking into account any ternary solid solubility and ternary compounds.
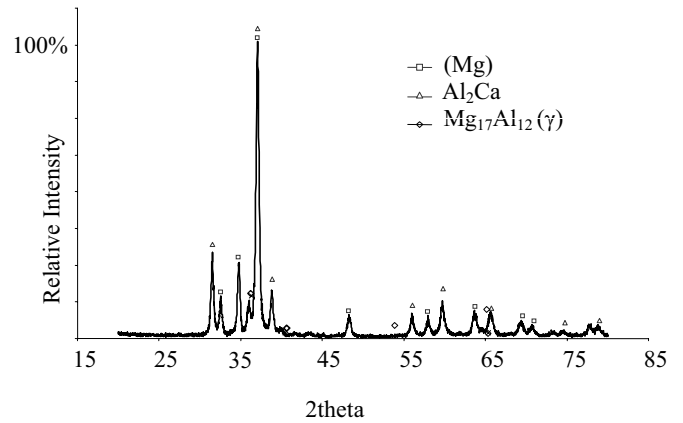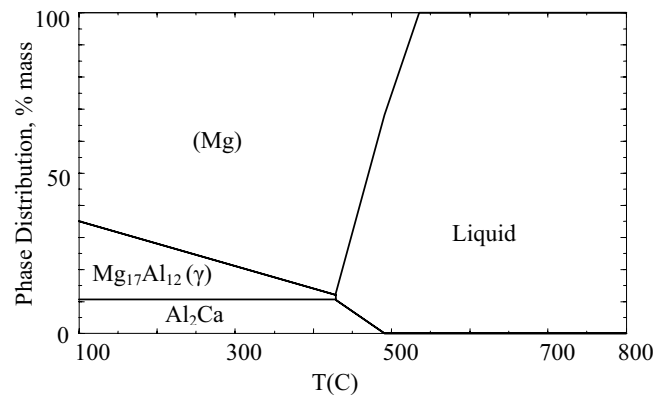
Figure 10: *X-ray diffraction patterns of sample 4.*

Figure 11: *Phase assemblage diagram of sample 3.*

It can be seen from Fig. 11 that Al_2Ca starts to precipitate at 485°C and was present at room temperature. However, the XRD pattern (Fig. 9) did not show the existence of this phase at room temperature. On the other hand, a phase with unknown peaks was detected and predicted as a ternary solid solution or a ternary intermetallic compound. The phase will be identified with crystal structure refinement in later investigation.
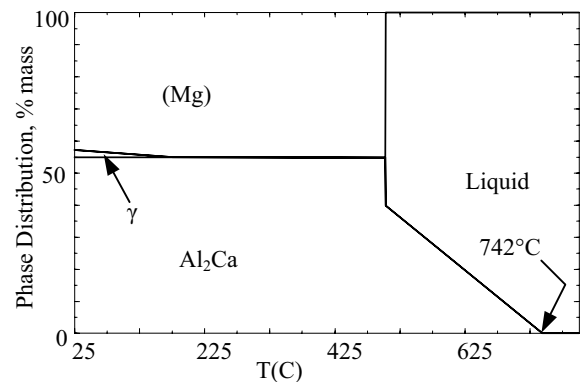
Figure 12: *Phase assemblage diagram of sample 4.*

Thermodynamic calculations of sample 4 (Fig. 12) shows that Al$_2$Ca phase started to solidify at 742°C, followed by (Mg) and γ phase. The proportion of γ phase is very low at room temperature, which has been reflected in terms of peak intensity in the diffraction pattern. It can be seen from Fig. 12 that the calculated liquidus for this sample is 742°C. This is quite close to the result obtained by the DSC. DSC measurements and the calculated thermal arrests along with phase field boundary are summarized in Table 5.

Table 5: *DSC measurements with thermodynamic analysis of Mg-Al-Ca alloys (h: denotes heating and c: denotes cooling).*

Sample	DSC Thermal Signals(°C)	Thermodynamic Prediction [Ref.18]	
		Temp.	Reactions
3	555h/550c	539	L / (Mg)+L
		485	(Mg)+L / Al$_2$Ca+(Mg)+L
	443h/431c	427	Al$_2$Ca+(Mg)+L / (Mg)+Al$_2$Ca+γ
4	760c	742	L / L+Al$_2$Ca
	535h/523c	504	L+Al$_2$Ca / Al$_2$Ca+(Mg)
	472h/443c		
		170	Al$_2$Ca+(Mg) / Al$_2$Ca+(Mg)+γ

Summary

The equilibria in Mg-Al-(Ca,Sr) systems have been investigated experimentally using DSC and XRD. A comparison with thermodynamic calculation is also presented. Some discrepancies between the experimental results and the thermodynamic predictions were observed as no ternary compounds or solid solutions are included in the thermodynamic models to date. However, there is an indication of ternary intermetallics or ternary solid solution in the investigated composition for each system. Further study is still needed on these systems in order to reveal the crystal structure and solubility limits of the ternary compounds/solid solutions and finally to provide more accurate phase diagrams for these systems.

Acknowledgements

References

[1] Pekguleryuz, M., Baril, E., Labelle, P. and Argo, D., Heat Resistant Mg Alloys for Powertrain Applications, Society of Automotive Engineers, [Special Publication], SP (2001). Journal of Advanced Materials – SAMPE, 35, 32-38, 2003.

[2] Blum, W., Watzinger, B., Grossman, B., and Haldenwanger, H.G., Comparative Study of Creep of the Die-cast Mg-alloys AZ91, AS21, AS41, AM60 and AE42, Materials Science and Engineering A, 319-321, 735-740, 2001.

[3] Emley, E.F., Principles of Magnesium Technology, Pergamon press, pp.483-542, 1966.

[4] Olivier B., The influence of Ca-Additions on the mechanical properties of T300-Cfibre/MG(Al) Metal Matrix Composites, Magnesium Alloys and their Applications, edit K.U. Kainer, pp, 215-220, 2000.

[5] Gruzleski, J.E. and Aliravci, Low porosity, Fine-Grain Sized Strontium Treated Magnesium Alloy castings, US Patent US005143564A, Sept. 1992.

[6] Aliravci, C. A., Gruzleski, J. E. and Dimayuga, F. C., AFS Transactions, pp. 92-115, 1992.

[7] Pekguleryuz, M., Creep Resistance in Mg-Al-Ca Casting Alloys, The Minerals, Metals & Materials Society (TMS), 12-17, 2000.

[8] Pekguleryuz, M., Baril, E., Labelle, P., and Argo, D., Creep Resistant Mg-Al-Sr Alloys, Journal of Advanced Materials–SAMPE, 35, 32-38, 2003.

[9] Chartrand, P., and Pelton, A.D., Critical Evaluation and Optimization of the Thermodynamic Properties and Phase Diagrams of the Al-Mg, Al-Sr, Mg-Sr and Al-Mg-Sr Systems, Journal of Phase Equilibria, 15(6), 591-605, 1994.

[10] Makhmudov, M.M., Vakhovob, A.V., and Dzhuraev, T.D., Liquidus Surface of Aluminum and Magnesium Phases of the Magnesium-Aluminum-Strontium Diagram, *Doklady Akademi Nauk Tadzhikskoi SSR*, 24(7), 435-438, 1981.

[11] Koray, O., Investigation in Mg-Al-Ca-Sr System by Computational Thermodynamic Approach Coupled with First-Principle Energetics and Experiments, PhD Thesis, The Pensylvenia State University, 2003.

[12] Baril, E., Labelle, P. and Pekguleryuz, M., Elevated Temperature Mg-Al-Sr: Creep Resistance, Mechanical Properties, and Microstructure, Journal of Materials, 55(11), 34-39, 2003.

[13] Gröbner, J., Kevorkov, D., Chumak, I. and Schmid-Fetzer, R., Experimental and Thermodynamic Calculation of Ternary Mg-Al-Ca Phase Equilibria, Zeitschrift fuer Metallkunde, 94, 976-982, 2003.

[14] Koray, O., Zhong, Y., Liu, Z.K., and Luo, A., Computational Thermodynamics and Experimental Investigation of the Mg-Al-Ca-Sr Alloys, Proceedings of the Minerals, Metals & Materials Society (TMS), 17-21, 69-73, February 2002.

[15] Powell, Bob R., Rezhets, V., Luo, A.A., and Tiwari, B.L., Creep-Resistant Magnesium Alloy Die Castings," US Patent No. 6,264,763 B1, dated July 24, 2001.

[16] Tkachenko, V.G., Khoruzhaya, V.G., Meleshevich, K.A., Karpets, M.V., and Frizel, V.V., Phase Equilibria in Mg-Al-Ca System, Powder Metallurgy and Metal Ceramics, 42 (5-6), 2003.

[17] Kraus, W., and Nolze, G., PowederCell for Windows, Version 2.3, Federal Institute of Materials Research and Testing, Berlin, 1999.

[18] Islam, F., Thermodynamic Modeling of the Mg-Al-Ca System, M.A.Sc. thesis, Mechanical and Industrial Eng. Dept., Concordia University, 2004.